Ribonucleoside-5′-diphosphates (NDPs) support RNA polymerase transcription, suggesting NDPs may have been substrates for primordial nucleic acid biosynthesis

Received for publication, April 25, 2019, and in revised form, May 21, 2019 Published, Papers in Press, June 12, 2019, DOI 10.1074/jbc.RA119.009074

Max E. Gottesman[‡] **and Arkady Mustaev**[§1]

From the [‡]*Department of Microbiology & Immunology, Columbia University Medical Center, New York, New York 10032 and* [§]*Public Health Research Institute and Department of Microbiology and Molecular Genetics, New Jersey Medical School, Rutgers Biomedical and Health Sciences, Newark, New Jersey 07103*

Edited by Patrick Sung

A better understanding of the structural basis for the preferences of RNA and DNA polymerases for nucleoside-5′-triphosphates (NTPs) could help define the catalytic mechanisms for nucleotidyl transfer during RNA and DNA synthesis and the origin of primordial nucleic acid biosynthesis. We show here that ribonucleoside-5′-diphosphates (NDPs) can be utilized as substrates by RNA polymerase (RNAP). We found that NDP incorporation is template-specific and that noncognate NDPs are not incorporated. Compared with the natural RNAP substrates, NTPs, the K_m of RNAP for NDPs was increased ~4-fold, whereas the V_{max} was decreased ~200-fold. These properties could be accounted for by molecular modeling of NTP/RNAP co-crystal structures. This finding suggested that the terminal phosphate residue in NTP (not present in NDP) is important for positioning the nucleotide for nucleolytic attack in the nucleotidyl transfer reaction. Strikingly, a mutational substitution of the active-center βR1106 side chain involved in NTP positioning also strongly inhibited NDP-directed synthesis, even though this residue does not contact NDP. Substitutions in the structurally analogous side chain in RB69 DNA polymerase (Arg-482) and HIV reverse transcriptase (Lys-65) were previously observed to inhibit dNDP incorporation. The unexpected involvement of these residues suggests that they affect a step in catalysis common for nucleic acid polymerases. The substrate activity of NDPs with RNAP along with those reported for DNA polymerases reinforces the hypothesis that NDPs may have been used for nucleic acid biosynthesis by primordial enzymes, whose evolution then led to the use of the more complex triphosphate derivatives.

Both NTPs and NDPs possess phosphoanhydride bonds that provide energy to direct biochemical reactions through coupling mechanisms. NTP and their deoxy derivatives are also utilized for nucleic acid biosynthesis by RNA and DNA polymerases, respectively (1). From an energetics standpoint, the choice for NTP substrates over NDPs for enzymatic polymerization reactions by these enzymes is not clear, because the free energy balance for the nucleotidyl transfer reaction for both of these compounds is similar. Thus, hydrolysis of the phosphoanhydride bonds in both NTP and NDP is driven by nearly the same Gibbs energy (2).

Understanding the structural basis for NTP preference by RNA and DNA polymerases helps to define the catalytic mechanisms for nucleotidyl transfer during RNA and DNA synthesis. In our previous study (3), we discovered a new activity of RNAP, phosphorolytic cleavage of nascent RNA transcript, which released 3′ terminal RNA residues in the form of NDPs. This reaction is functionally analogous to pyrophosphorolysis, which yields NTPs as reaction products (4). Because pyrophosphorolysis is a reversal of RNA synthesis based on nucleotidyl transfer from NTP substrates, we reasoned that NDPs might also serve as substrates for RNA synthesis. Previous reports testing labeled NDPs (5, 6) in crude transcription assays revealed some residual incorporation of radioactive nucleotide material into acid-insoluble products in the presence of RNAP and DNA templates. However, it was not clear if this incorporation was because of traces of NTPs in the NDP preparations. In the present study, we used highly purified NDPs to examine their substrate activity with RNAP in an arsenal of biochemical transcription assays and mutational analyses. We find that NDPs can be utilized as substrates for transcription by RNAP, albeit less efficiently than NTP substrates. Previous studies with DNA polymerases (7, 8) and reverse transcriptase (9) detected substrate activity of NDPs with these enzymes. Our data, along with the results of these studies, is consistent with the hypothesis that the simpler NDPs may have emerged earlier than NTPs and were utilized as substrates by nucleic acid polymerases at early steps in the origin of life. This is supported by the ability of a currently existing enzyme, polynucleotide phosphorylase (PNP) to utilize efficiently NDP for non–template-encoded RNA synthesis.

Results

NDPs are substrates for Escherichia coli RNA polymerase

We first asked if NDPs could extend RNA primers in ternary elongation complexes (TEC)[2] assembled from RNAP and synthetic oligonucleotides. We constructed TEC containing a 9-nucleotide RNA and then elongated it with the next cognate

This work was supported by internal Public Health Research Institute support grant (to A.M.) and by National Institutes of Health Grant R01 GM037219 (to M.G.). The authors declare that they have no conflicts of interest with the contents of this article. The content is solely the responsibility of the authors and does not necessarily represent the official views of the National Institutes of Health.

[1] To whom correspondence should be addressed. E-mail: mustaear@njms.rutgers.edu.

[2] The abbreviations used are: TEC, ternary elongation complex; RNAP, RNA polymerase; PNP, polynucleotide phosphorylase; DNAP, DNA polymerase; TB, transcription buffer.

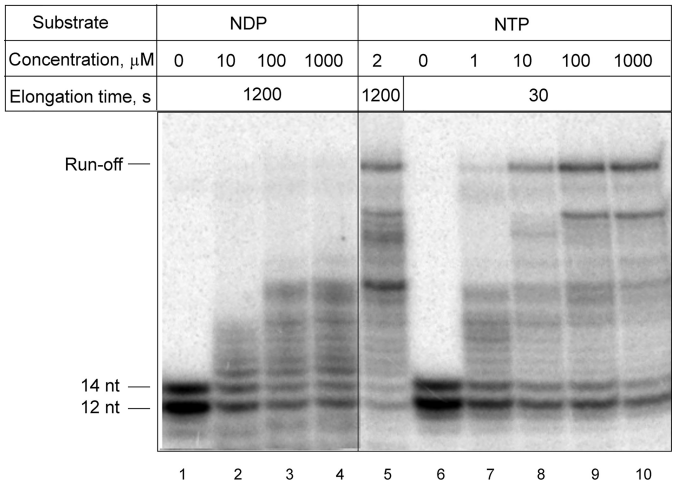

Figure 1. RNA elongation by NDP and NTP in TEC12 under various substrate concentrations. The substrate concentration, incubation time, positions of the original RNA primer, and run-off transcript are indicated.

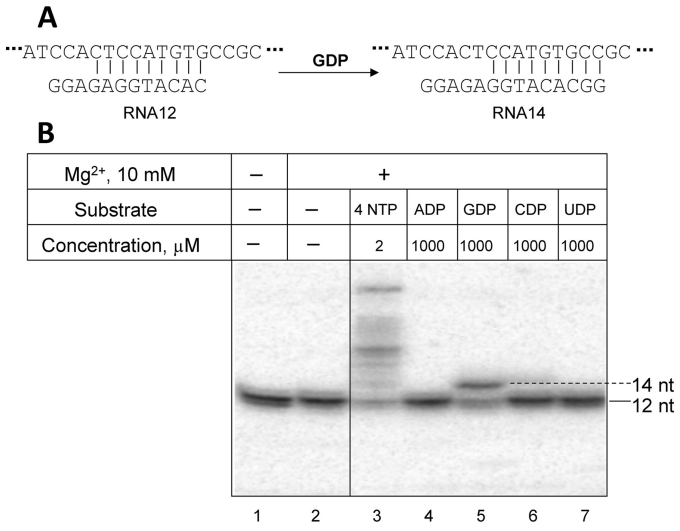

Figure 2. Elongation of RNA primer in TEC12 by NDP substrates under various incubation conditions. *A*, the scheme of the RNA12 elongation by GDP. *B*, electrophoretic separation of the reaction products. Substrate concentrations and the positions of original RNA12 and elongation products are indicated.

substrate, [α-^{32}P]CTP. The resulting radiolabeled TEC10 was further extended to TEC12, which was used to probe the substrate activity of NDPs. As seen in Fig. 1, incubation of TEC12 with the mixture of four NDPs reduced the amount of the original 12-nucleotide RNA and led to the appearance of longer RNAs. Increasing NDP concentrations yielded progressive increases in RNA lengths (Fig. 1, *lanes 2–4*). These results demonstrate that NDPs are active RNAP substrates. To examine the template specificity of this RNA synthesis, we challenged TEC12 with various NDPs (Fig. 2, *lanes 4–7*). Only the cognate GDP promoted RNA extension, indicating that NDP incorporation is template-specific.

The K_m values of NDPs and NTPs are comparable, but the NDP V_{max} is significantly reduced.

As seen from Fig. 1, for both NDP and NTP, the rate of RNA synthesis progressively increased up to a nucleotide concentration 100 μM, whereupon a plateau was reached (compare *lanes 2–4* with *8–10* of Fig. 1). This result indicates that the K_m values for NDPs and NTPs are comparable. For a more precise determination of the catalytic parameters of these substrates, we assayed them in a single-nucleotide RNA extension assay in TEC10. RNA elongation of TEC10 by ATP proceeds unusually slow, thus obviating the need in fast kinetics devices for K_m and V_{max} determination. As seen in Table 1 and Fig. 3, *A* and *D*, consistent with the experiment described above (Fig. 1) the K_m values of ATP and ADP were roughly equivalent (20 μM and 80 μM, respectively). Remarkably, a similar correspondence in dissociation constants (K_d) for UDP and UTP from the RNAP active center (5-fold) has been reported (10), confirming that interactions of the NTP γ-phosphate do not contribute significantly to active center binding. However, as shown in Table 1 and Fig. 3*D*, the V_{max} was about 200-fold lower for ADP compared with ATP, reflecting a significant contribution of the NTP terminal phosphate to the catalysis. This difference in V_{max} corresponds to a ~3 kcal/mol decrease in activation energy for ATP compared with ADP. To provide independent evidence for this calculation, we determined the activation energy for ADP and ATP incorporation by measuring the incorporation rate at various temperatures (Fig. 4). Activation energies for ADP and ATP according to the Arrhenius equation were 21.6 and 17.6 kcal/mol respectively. The difference ~4 kcal/mol is in good agreement to that suggested from the difference in V_{max} determined in the previous assay. Notably, the activation energy for ADP in RNAP nucleotidyl transfer (~22 kcal/mol) is close to that for dADP (25 kcal/mol) determined in DNA polymerization with Taq enzyme (8).

Effect of Mn^{2+} ions on the rate of single-step NDP and NTP incorporation

Mn^{2+} ions increase the rate of RNA synthesis of modified NTPs with poor substrate capacity (11) as well as with natural NTP substrates. Stimulation is more pronounced with a mixture of Mn^{2+} and Mg^{2+} ions (11). Moreover, Mn^{2+} can suppress inhibition by active RNAP center mutations (12–15). This effect of Mn^{2+} is attributed to stronger substrate coordination at the active center by the metal ion, which facilitates formation of the reaction transition state. We therefore asked whether Mn^{2+} can stimulate RNA synthesis with NDPs in lieu of Mg^{2+}. We examined the effect of these two metal ions alone and together on nucleotidyl transfer with ATP and ADP in TEC10. As shown in Fig. 5, Mn^{2+} alone, or mixed with Mg^{2+}, significantly (~2-fold) increased the rate of ATP incorporation. Importantly, we saw no stimulation of ADP incorporation by Mn^{2+}. This result is explained by our molecular models (see below).

Molecular modeling of the NDP polymerization reaction

Notably, there are no high-resolution structures of RNAP with an NTP substrate bound to the active center in a catalytically competent mode consistent with the S_n2 reaction mechanism (12, 16–21). Thus in the 1R9S structure of the yeast pol II enzyme (16), the NTP β-phosphate does not coordinate with either of the Me^{2+} ions of the active center, whereas this coordination is seen in all relevant structures of DNAP-NTP com-

TABLE 1
Steady-state kinetic parameters of nucleic acid polymerases with NTP and NDP substrates
Data for RB69 DNAP, Taq DNAP, and HIV RT are from Refs. 7, 8, and 9, respectively.

E. coli RNAP (20° C)

	WT			βK1073A			βR1106A		
	K_m, μM	V_{max}, s^{-1}	V_{max}/K_m	K_m, μM	V_{max}, s^{-1}	V_{max}/K_m	K_m, μM	V_{max}, s^{-1}	V_{max}/K_m
ATP	20	1.53	7.7×10^{-2}	2.2	1.4×10^{-3}	6.4×10^{-4}	100	2×10^{-3}	2×10^{-5}
ADP	80	1.1×10^{-2}	1.4×10^{-4}	200	9.2×10^{-5}	4.6×10^{-7}	300	1.4×10^{-5}	4×10^{-8}
ATP/ADP ratio	0.25	140	550	0.011	15	1400	0.33	143	500

DNAP RB69 (25° C)

	WT			K560A			R482A		
	K_m, μM	V_{max}, s^{-1}	V_{max}/K_m	K_m, μM	V_{max}, s^{-1}	V_{max}/K_m	K_m, μM	V_{max}, s^{-1}	V_{max}/K_m
dCTP	69	200	2.9	790	0.8	1.0×10^{-3}	1100	3.3	4.6×10^{-2}
dCDP	1200	0.5	4.2×10^{-4}	1800	1.4×10^{-3}	7.7×10^{-7}	140	1.6×10^{-3}	1.1×10^{-5}
ATP/ADP ratio	0.058	400	6900	0.44	571	1300	7.86	2062	4180

HIV RT (37° C)

	K_m, μM	V_{max}, s^{-1}	V_{max}/K_m
dATP	0.02	0.038	1.9
dADP	9.9	3.3×10^{-4}	3.3×10^{-5}
ATP/ADP ratio	0.002	115	5.7×10^4

Taq DNAP (72° C)

	K_m, μM	V_{max}, s^{-1}	V_{max}/K_m
dATP	20	47	2.35
dADP	420	6	1.4×10^{-2}
ATP/ADP ratio	0.048	7.8	168

plexes (Fig. 6, *C* and *D*). In the structure of *Thermus thermophilus* RNAP (22), the coordination of the NTP by active center Mg^{2+} ions is severely distorted, possibly reflecting a catalytically inactive intermediate state. To explain our results, therefore, we used our previously constructed model (18), in which the NTP triphosphate chain position was adjusted to that seen in the DNAP complexes (Fig. 6), on the premise that both enzymes operate by a universal S_n2 catalytic mechanism. In this model, the triphosphate chain of the bound NTP makes a set of contacts with two active center Me^{2+} ions and with side chains of the basic β subunit Lys-1073, Arg-1106 and Arg-678 residues of RNAP (Fig. 6*A*). This configuration of the triphosphate chain is stabilized by α-phosphate coordination with Mg-I, and by β- and γ-phosphate coordination with Mg-II, as well as by electrostatic/hydrogen-bonding interaction of γ-phosphate with βLys-1073, βArg-678, and βArg-1106. In this arrangement the α-phosphate group is poised for nucleophilic attack by the 3′ hydroxyl of the terminal RNA residue (shown as a *red sphere* in Fig. 6, *A* and *B*), so that the directions of the attack and the release of the leaving pyrophosphate group are aligned in the transition state. Next, we built a model for active center–bound NDP by eliminating the γ-phosphate residue from the previous structure (Fig. 6*B*). In the absence of the constraints imposed by interactions of the terminal γ-phosphate residue in the NTP-TEC complex, the β-phosphate can readily change its conformation to acquire additional energetically favorable contacts. Thus it can simultaneously coordinate to Mg-II through two oxygens and engage the amino group of βLys-1073 side chain, which would change the side chain conformation seen in the NTP complex to approach the NDP terminal phosphate. This acquisition of new contacts is consistent with the subtle change in K_m value for NDP compared with NTP. However, this NDP diphosphate chain rearrangement would misalign the reactant groups (Fig. 6*B*), and thus adversely affect catalysis. This distortion can explain the dramatic decrease in V_{max} for NDP compared with NTP (see Table 1).

The NDP binding model can also account for the different effects of Mn^{2+} on the NDP and NTP nucleotidyl transfer reactions. Because the orientation of the reactant groups in nucleotidyl transfer is suboptimal with NDP due to the change in β-phosphate coordination, it is expected that the reaction proceeds more efficiently in the correct NDP coordination state

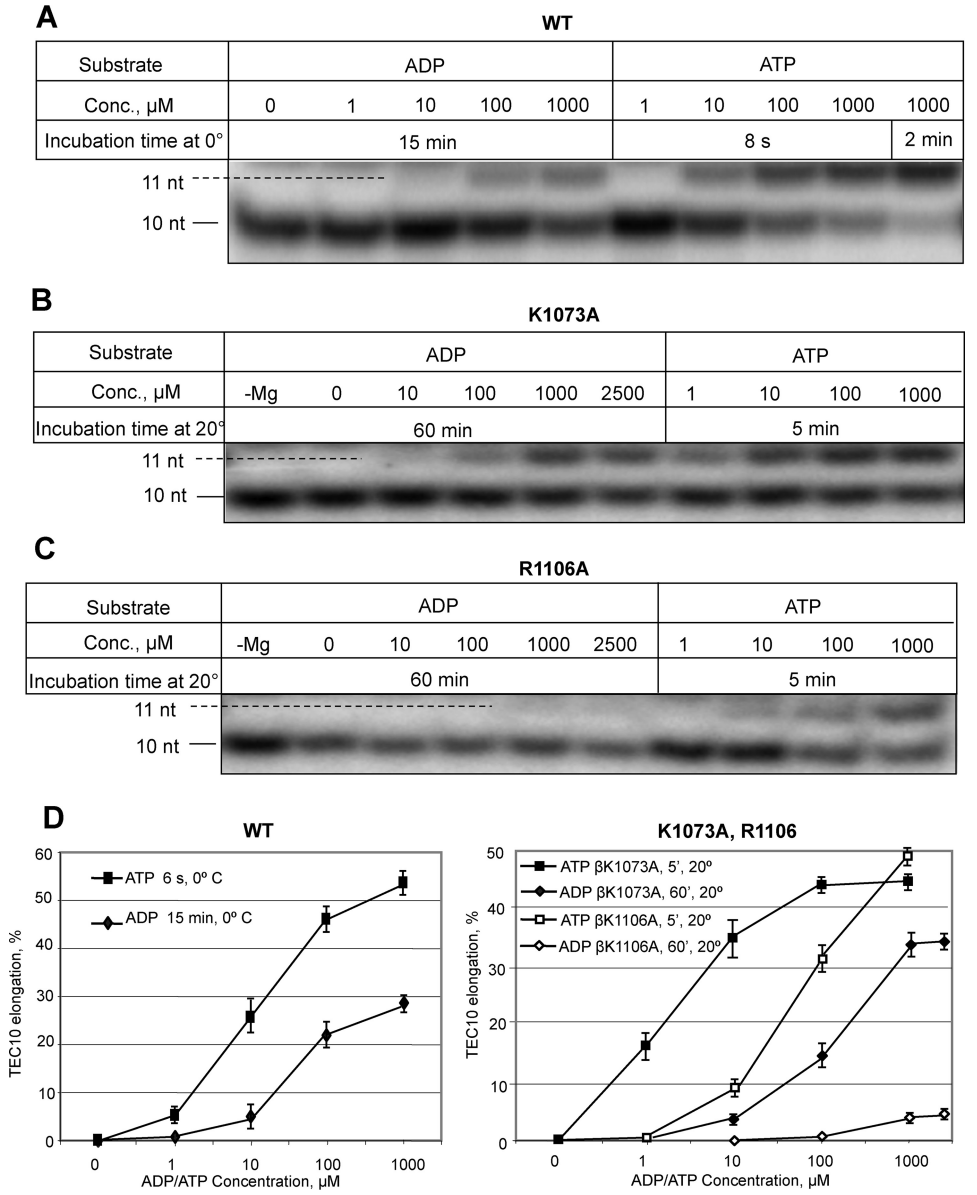

Figure 3. Single-step elongation of RNA in TEC10 by ADP and ATP with WT (*A*) and mutant (*B* and *C*) RNAP. The positions of original RNA10 and the extended RNA 11 product are indicated. *D*, graphical representation of the results of *A*–*C*.

observed with NTP (Fig. 6*A*), which can exist in equilibrium with suboptimal orientations. The enhancement of NTP incorporation by Mn^{2+}, because of the stronger coordination of the attacking 3′ RNA hydroxyl group and α-phosphate group compared with Mg^{2+}, might be negated by β-phosphate coordination with the Mn-II ion. The stronger coordination by Mn^{2+} would reduce NDP incorporation by shifting the coordination equilibrium toward the substrate suboptimal orientation, thus nullifying enhancement by Mn-I.

Effects of active center mutations on NDP/NTP incorporation

As shown in Fig. 6, βLys-1073, βArg-1106 are the residues closest to the active center-bound NTP/NDP substrates and are likely to participate in catalysis. We therefore investigated the effect of alanine substitutions of these residues on nucleotidyl transfer catalysis. The βK1073A mutation increased the K_m 2.5-fold for NDP in single-step elongation of TEC10 (Fig. 3, *B* and *D*, and Table 1), in accord with the proposed involvement of this residue in NDP retention at the active center (Fig. 6*B*). The substitution also caused a ~100-fold reduction in the maximal reaction rate. Surprisingly, the βLys-1073 mutation enhanced NTP binding ~10-fold, while decreasing V_{max} ~500-fold (Fig. 3, *B* and *D*, and Table 1). The reduced K_m by the substitution is puzzling and was not previously observed in testing of this mutant with promoter templates (23). We suggest that the reduction in K_m might be specific to TEC10. In our previous study (3) we demonstrated that TEC10 is mostly pretranslocated. Thus, the substitution might influence the NTP K_m indirectly by affecting RNAP translocation equilibrium. The βR1106A substitution moderately increased K_m for both ADP and ATP (2.5- and 5-fold, respectively) but reduced the maximal incorporation rate ~800-fold for both substrates (Fig. 3, *C* and *D*, and Table 1). Altered substrate retention in the mutant enzyme for ATP can be explained by elimination of the

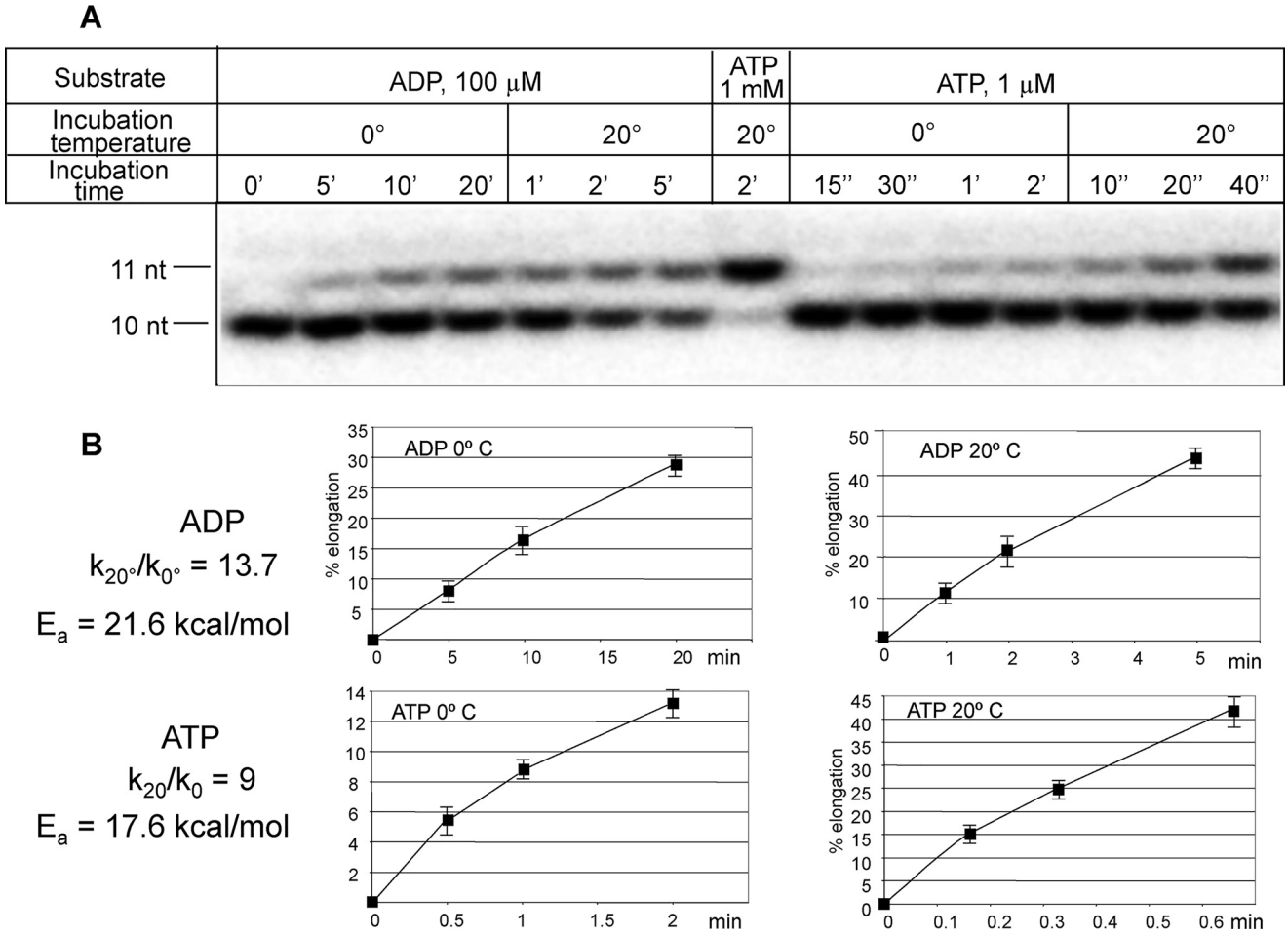

Figure 4. Determination of the activation energy for ATP and ADP elongation of RNA in TEC10. *A*, separation of the radioactive elongation products after incubation under various conditions. *B*, quantification of the elongation products.

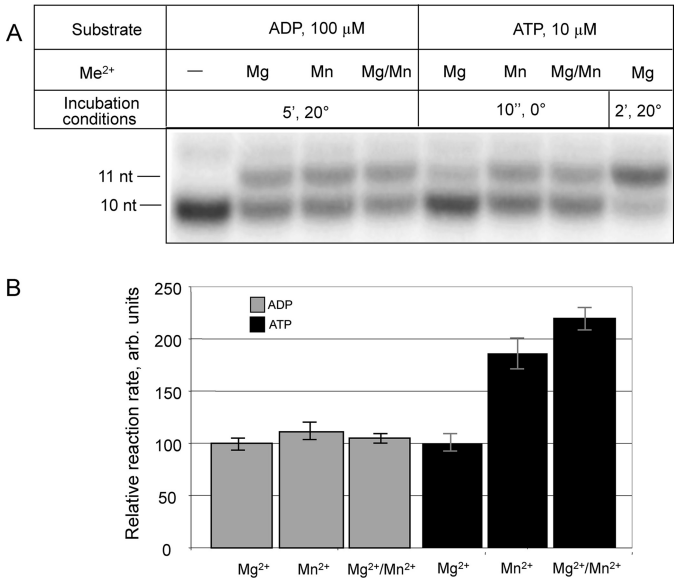

Figure 5. Single-step elongation of RNA in TEC10 by ADP and ATP in the presence of Mg^{2+} and Mn^{2+}. *A*, separation of the radioactive reaction products (representative gel). *B*, quantification of the results of *A*. *Error bars* represent S.D. from four independent experiments.

salt bridge between the Arg guanidine group and ATP γ-phosphate. The effect of the substitution on ADP K_m could reflect long-range electrostatic interactions between the substrate and the βArg-1106 side chain. Because this side chain does not contact ADP (Fig. 6*B*), why βArg-1106 reduces the maximal reaction rate of ADP cannot be easily explained. We return to this point below.

Discussion

We find that NDPs can be used, although less efficiently than NTPs, as substrates by RNA polymerase. Together with previous observations (7–9) this finding demonstrates that NDP utilization is a common property of nucleic acid biosynthetic enzymes. Molecular modeling performed in this study and analysis of X-ray structures provide a rationale for our data. Specifically, our model explains why NDP incorporation into RNA is less efficient than NTP incorporation. The terminal phosphate of an NTP substrate makes important interactions with RNAP active center side chains that contribute to substrate retention and pose the substrate for catalysis. This explains the increase in K_m and the drastic decrease in V_{max} for NDP relative to NTP. Notably, compared with RNAP, the dNDP/dNTP K_m ratio increases more dramatically (Table 1) for DNA polymerases (about 20-fold with RB69 and TaqDNAP and about 500-fold with HIV RT). The striking increase in K_m in

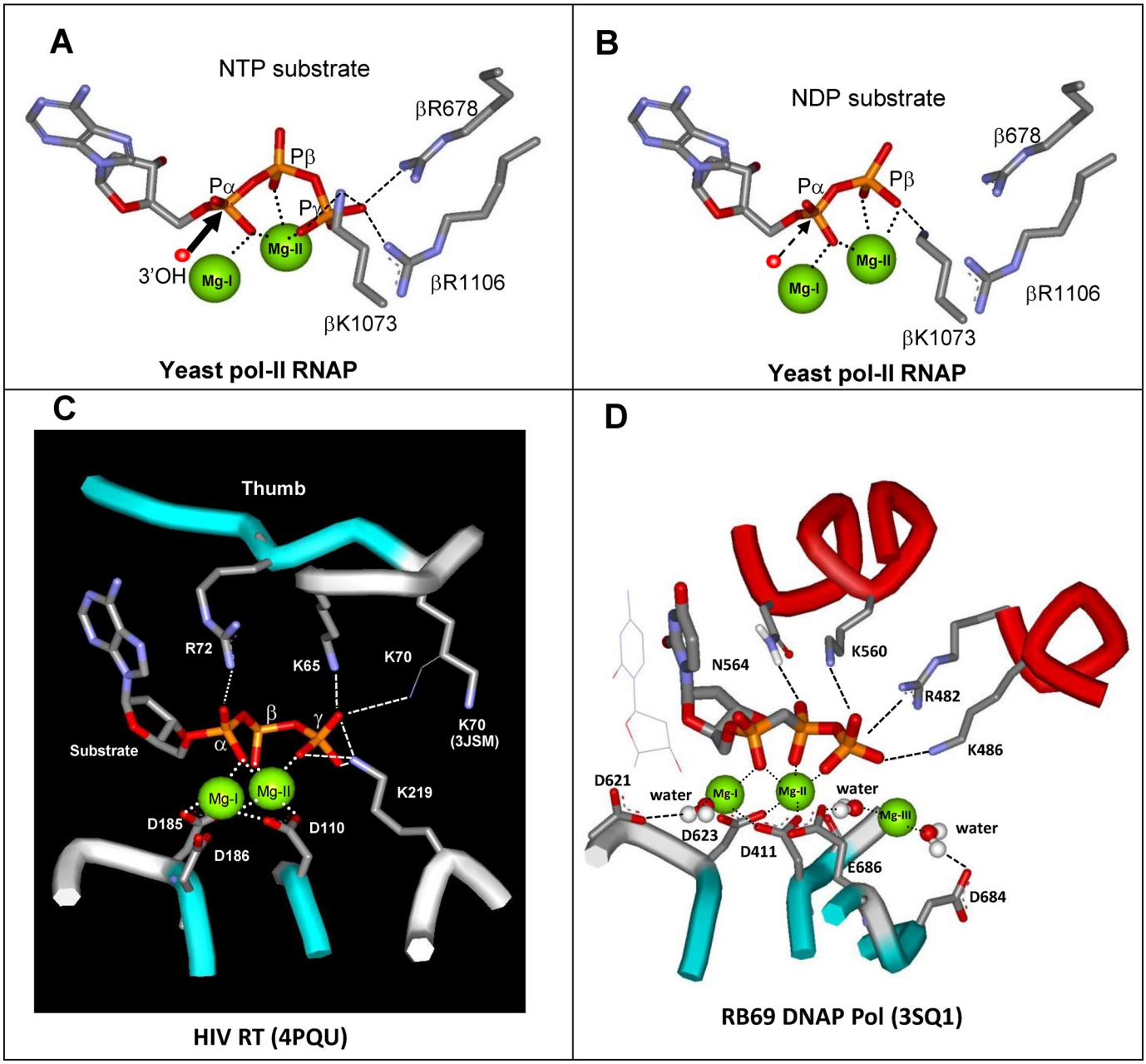

Figure 6. Molecular images for nucleotide substrates bound to nucleic acid polymerases. *A* and *B*, RNAP TEC with NTP and NDP substrates, respectively. Nucleotide substrates and active center side chains are shown in *stick* rendition, and Mg^{2+} ions in Corey-Pauling-Koltun (*CPK*) rendition. *Arrows* indicate the direction of nucleophilic attack of the 3′RNA hydroxyl group (*red sphere*) on NTP α–phosphate during nucleotidyl transfer. *Dotted lines* show coordination bonds; *dashed lines*, salt bridges and hydrogen bonds. The active center site chains are indicated. *C* and *D*, substrate interactions in the active center of HIV RT and RB69 DNAP, respectively.

the case of HIV RT can be explained by extensive interactions of the dNTP γ-phosphate with HIV RT active center residues Lys-65, Lys-70, and Lys-219 (Fig. 6*C*). These are lost with an NDP substrate. Molecular modeling of other polymerizing enzymes suggests that some of the active center residues interacting with the NTP γ-phosphate can also salt bridge to the NDP β–phosphate-βLys-1073 in RNAP and likely Lys-560 in RB69 DNAP. These contacts could account for the more moderate increase in NDP K_m.

The maximal reaction rate with NDP for all polymerases is also slower than that with NTP, which reflects the role of the NTP terminal phosphate interactions in lowering the reaction activation barrier. Thus the strongest V_{max} drop was observed with RB69 DNAP (400-fold) followed by RNAP (140-fold), HIV RT (115-fold), and TaqDNAP (~8-fold). The smaller difference between the dNTP- and dNDP-directed reactions with the Taq enzyme could be because of the high reaction temperature (72 °C) used in the assay. In fact, incorporation of dNDP is more temperature-dependent than dNTP incorporation. This is because of the higher activation energy of nucleotidyl transfer from dNDPs compared with that from natural substrates. Thus, the difference between dNTP and dNDP incorporation rates is smaller at higher than at lower temperatures.

The relative efficiency of NDP substrates can be expressed as the ratio of the maximal reaction rate to K_m. As seen in Table 1, the drop in V_{max}/K_m ratio for NDP relative to NTP was about 550-fold for RNAP. This value is comparable with that for TaqDNAP (168-fold) (9), but much less than that for RB69 DNAP (6900-fold) (7), and HIV RT (5.7×10^4-fold) (10).

The effects of substitution of the positively charged active center residues bracketing the nucleotide substrates on the NDP *versus* NTP incorporation rates provide insight into the mechanism of polymerization catalysis. Thus, alanine substitutions of *E. coli* RNAP βLys-1073 and βArg-1106 residues strongly reduced catalysis with both NTP and NDP substrates. These residues interact with the γ-phosphate of NTP. The significant decrease in catalytic efficiency of NTP with the βR1106A substitution is less obvious with NDP; this residue does not contact NDP. A reduced catalytic efficiency was observed when the structurally analogous Lys-560 and Arg-482 residues in RB69 DNAP were mutated (see Fig. 6*D* and Table 1). Similarly, mutations in HIV RT Lys-65, which forms a salt bridge with NTP γ-phosphate, but is not in a contact with the bound NDP β-phosphate (see Fig. 6*C*), marginally reduces NTP catalysis (9) but completely abolishes NDP incorporation. Notably, the mutant enzyme retained the ability to bind NDP. These findings define a common catalytic factor involved in phosphodiester bond formation by nucleic acid polymerases that is not mediated through immediate contacts of the active center residues with NDP and, possibly, NTP. These residues might play a role in active center dynamics accompanying catalysis that escapes the resolution of crystallographic analysis, or in an intermediate state of substrate binding. Thus, despite the loss of the catalytic performance with NDP compared with natural NTP substrates for all of the tested enzymes, the activity of NDPs is sufficient to support nucleic acid biosynthesis.

Structurally, NDPs are simpler compounds than NTPs and may have been biosynthesized prior to NTPs at earlier steps of evolution. Like NTPs, NDPs are energy-rich phosphoanhydrides. Importantly, the hydrolysis of a phosphoanhydride bond in both di- and triphosphate compounds provides a comparable amount of energy, suggesting that NDPs could efficiently substitute for NTPs in virtually all biochemical reactions that rely on a supply of high energy, including phosphoryl and nucleotidyl transfer.

NDPs substrate activity with RNAP reported here is consistent with the idea that during the development of life on Earth NDPs might have played significant roles in support of many biochemical reactions, including nucleic acid biosynthesis. Notably, NDPs are more resistant to hydrolytic cleavage at high temperature than NTPs, because they contain only one phosphoanhydride bond. This might have been a significant factor in maintaining the pool of these molecules at the elevated temperatures in which first living systems evolved.

The substrate activity of NDPs with single-subunit RNAP of phage and mitochondrial origin has yet to be explored. The possibility of NDP to support RNA synthesis by these enzymes comes from high structural homology of their active center with that of DNAP.

That NDPs could support efficient polymerization stems from the precedent of polynucleotide phosphorylase (24), which releases P_i as its reaction product. Unlike PNP, however, nucleotide polymerization with NTPs or dNTPs by RNAP or DNAP is not readily reversible because the pyrophosphate reaction product is rapidly cleaved by inorganic pyrophosphatase, which maintains a low micromolar level of intracellular pyrophosphate concentration (25). In contrast, NDP polymerization yields P_i, whose concentration in the cell is high, about 0.01–0.1 M (26, 27). Therefore, in the cell PNP readily catalyzes RNA phosphorolysis, the reverse reaction to NDP polymerization, which releases NDP products. These considerations support the idea that the introduction of NTPs in the cellular metabolome might allow more efficient synthesis of nucleic acids by rendering polymerization irreversible.

Experimental procedures

All chemicals were from Sigma-Aldrich. His_6-tagged RNA polymerase was purified from the RL721 *E. coli* strain. Ultrapure ribo- and 2′-deoxynucleoside-5′-triphosphates (NTPs, dNTPs) were from Pharmacia. Ribo- and 2′-deoxynucleoside-5′-diphosphates (NDP and dNDP) (Sigma-Aldrich) were purified by preparative thin layer chromatography (TLC) in dioxane-isopropanol-25% ammonium hydroxide-water (1:1:1:1) developing system followed by column chromatography on Dowex 1 × 8, 400 mesh in LiCl gradient. RNAP mutants were prepared as described previously (14). [α-^{32}P]CTP was from MP Biomedicals. Oligonucleotides were from Integrated DNA Technologies. DNA template strand was 5′-ACCAGCAGGCCGATTGGGATGGGTATTCGCCGTGTACCTCTCCTAGCCCCCAAGTATCCTATAGG-3′. DNA nontemplate strand was 5′-CCTATAGGATACTTGGGGGCTAGGAGAGGTACACGGCGAATACCCATCCCAATCGGCCTGCTGGT-3′. RNA9A was 5′ GGAGAGGUA 3′.

Polyuridylic acid was from Sigma. Radioactive products were resolved by electrophoresis in 20% PAAG in the presence of 7 M urea and quantified by phosphoimagery using a Molecular Dynamics device (GE Healthcare) and Storm 60 software. Molecular modeling was performed using WebLab Viewer-Light 4.0 (Molecular Simulations Inc.). The experiments described below were repeated three times, unless specified otherwise.

Elongation complexes

TEC9A was assembled as described previously (3). Briefly, RNA9 was mixed with equivalent amounts of DNA template strand to final concentration of 1 μM in transcription buffer (TB) (20 mM Tris-HCl, pH 8.0, 0.1 M NaCl, 10 mM $MgCl_2$) at 40 °C and left to cool in a water bath to room temperature for ~30 min. This mixture was added to an equivalent amount of His_6-tagged RNAP immobilized on nitrilotriacetic acid (NTA) agarose and kept at room temperature in a shaker for 10 min followed by addition of the equivalent amount of DNA nontemplate strand. The mixture was agitated for another 10 min at room temperature and supplemented with TB containing 1 M NaCl. The pellet was separated and washed with regular TB. If required, the TEC was further elongated to TEC11 by subsequent incubation with 1 μM CTP and 50 μM ATP (each incubation 20 min, 0 °C in TB containing 1 mM $MgCl_2$). Labeled TEC10C, and TEC12C, were obtained by elongation of TEC9A

or TEC11A by an equivalent amount of [α-^{32}P] CTP (3000 Ci/mmol, 10 mCi/ml; MP Biomedicals) for 2 min at ambient temperature followed by washing with TB (4 × 1 ml).

Elongation of TEC12 in the presence of NDP and NTP

The elongation reactions (20 min, 20 °C) were performed in TB using NDP/NTP concentrations indicated in Figs. 1 and 2. Control mixtures lacked NDP/NTP or $MgCl_2$. The reactions were initiated by addition of $MgCl_2$ and stopped by mixing with equal volume of 10 M urea, 50 mM EDTA, pH 8.0.

Single nucleotide elongation of TEC10C by ADP and ATP

This was performed in TB under the conditions indicated in Figs. 3 and 4. The reactions were started and terminated as described above.

Effect of Mn^{2+} on ATP and ADP incorporation in TEC10C

TEC10C in TB lacking Mg^{2+} was supplied with 100 μM ADP or 10 μM ATP and the reaction started by addition of Mg^{2+} (1 mM), Mn^{2+} (0.2 mM), or Mg^{2+}/Mn^{2+} (1 mM, 0.2 mM, respectively). After incubation at the conditions specified in Fig. 5, the reaction was stopped as described above.

Author contributions—M. E. G. and A. M. conceptualization; M. E. G. writing-review and editing; A. M. investigation; A. M. methodology; A. M. writing-original draft; M. E. G. experiments and results discussion.

References

1. Dikson, M., and Webb, E. C. (1979) *Enzymes*, 3rd ed., Longman Publishing Group, New York, NY
2. Alberty, R. A., and Goldberg, R. N. (1992) Standard thermodynamic formation properties for the adenosine 5′-triphosphate series. *Biochemistry* **31,** 10610–10615 CrossRef Medline
3. Gottesman, M. E., and Mustaev, A. (2018) Inorganic phosphate, arsenate, and vanadate enhance exonuclease transcript cleavage by RNA polymerase by 2000-fold. *Proc. Natl. Acad. Sci. U.S.A.*, **115,** 2746–2751 CrossRef Medline
4. Rozovskaya, T. A., Rechinsky, V. O., Bibilashvili, R. S., MYa, K., Tarusova, N. B., Khomutov, R. M., and Dixon, H. B. (1984) The mechanism of pyrophosphorolysis of RNA by RNA polymerase. Endowment of RNA polymerase with artificial exonuclease activity. *Biochem. J.* **224,** 645–650 CrossRef Medline
5. Chamberlin, M., and Berg, P. (1962) Deoxyribonucleic acid-directed synthesis of ribonucleic acid by an enzyme from *Escherichia coli*. *Proc. Natl. Acad. Sci. U.S.A.* **48,** 81–94 CrossRef Medline
6. Furth, J. J., Hurwitz, J., and Anders, M. (1962) The role of deoxyribonucleic acid in ribonucleic acid synthesis. I. The purification and properties of ribonucleic acid polymerase. *J. Biol. Chem.* **237,** 2611–2619 Medline
7. Yang, G., Franklin, M., Li, J., Lin, T.-C., and Konigsberg, W. (2002) Correlation of the kinetics of finger domain mutants in RB69 DNA polymerase with its structure. *Biochemistry* **41,** 2526–2534 CrossRef Medline
8. Burke, C. R., and Lupták, A. (2018) DNA synthesis from diphosphate substrates by DNA polymerases. *Proc. Natl. Acad. Sci. U.S.A.* **115,** 980–985 CrossRef Medline
9. Garforth, S. J., Parniak, M. A., and Prasad, V. R. (2008) Utilization of a deoxynucleoside diphosphate substrate by HIV reverse transcriptase. *PLoS One* **3,** e2074 CrossRef Medline
10. Szafrański, P., 2nd, Smagowicz, W. J., and Wierzchowski, K. L. (1985) Substrate selection by RNA polymerase from *E. coli*. The role of ribose and 5′-triphosphate fragments, and nucleotides interaction. *Acta Biochim. Pol.* **32,** 329–349 Medline
11. Kozlov, M., Bergendahl, V., Burgess, R., Goldfarb, A., and Mustaev, A. (2005) Homogeneous fluorescent assay for RNA polymerase. *Anal. Biochem.* **342,** 206–213 CrossRef Medline
12. Sosunov, V., Zorov, S., Sosunova, E., Nikolaev, A., Zakeyeva, I., Bass, I., Goldfarb, A., Nikiforov, V., Severinov, K., and Mustaev, A. (2005) The involvement of the aspartate triad of the active center in all catalytic activities of multisubunit RNA polymerase. *Nucleic Acids Res.* **33,** 4202–4211 CrossRef Medline
13. Copeland, W. C., and Wang, T. S. (1993) Mutational analysis of the human DNA polymerase α. The most conserved region in α-like DNA polymerases is involved in metal-specific catalysis. *J. Biol. Chem.* **268,** 11028–11040 Medline
14. Saturno, J., Lázaro, J. M., Blanco, L., and Salas, M. (1998) Role of the first aspartate residue of the "YxDTDS" motif of ϕ29 DNA polymerase as a metal ligand during both TP-primed and DNA-primed DNA synthesis. *J. Mol. Biol.* **283,** 633–642 CrossRef Medline
15. Pritchard, A. E., and McHenry, C. S. (1999) Identification of the acidic residues in the active site of DNA polymerase III. *J. Mol. Biol.* **285,** 1067–1080 CrossRef Medline
16. Westover, K. D., Bushnell, D. A., and Kornberg, R. D. (2004) Structural basis of transcription: Nucleotide selection by rotation in the RNA polymerase II active center. *Cell* **119,** 481–489 CrossRef Medline
17. Steitz, T. (1998) A mechanism for all polymerases *Nature* **391,** 231–232 CrossRef Medline
18. Sosunov, V., Sosunova, E., Mustaev, A., Bass, I., Nikiforov, V., and Goldfarb, A. (2003) Unified two-metal mechanism of RNA synthesis and degradation by RNA polymerase. *EMBO J.* **22,** 2234–2244 CrossRef Medline
19. Sosunova, E., Sosunov, V., Kozlov, M., Nikiforov, V., Goldfarb, A., and Mustaev, A. (2003) Donation of catalytic residues to RNA polymerase active center by transcription factor Gre. *Proc. Natl. Acad. Sci. U.S.A.* **100,** 15469–15474 CrossRef Medline
20. Kettenberger, H., Armache, K. J., and Cramer, P. (2003) Architecture of the RNA polymerase II-TFIIS complex and implications for mRNA cleavage. *Cell* **114,** 347–357 CrossRef Medline
21. Opalka, N., Chlenov, M., Chacon, P., Rice, W. J., Wriggers, W., and Darst, S. A. (2003) Structure and function of the transcription elongation factor GreB bound to bacterial RNA polymerase. *Cell* **114,** 335–345 CrossRef Medline
22. Vassylyev, D. G., Vassylyeva, M. N., Zhang, J., Palangat, M., Artsimovitch, I., and Landick, R. (2007) Structural basis for substrate loading in bacterial RNA polymerase. *Nature* **448,** 163–168 CrossRef Medline
23. Sagitov, V., Nikiforov, V., and Goldfarb, A. (1993) Dominant lethal mutations near the 5′ substrate binding site affect RNA polymerase propagation. *J. Biol. Chem.* **268,** 2195–2202 Medline
24. Grunberg-Manago, M., Ortiz, P., and Ochoa, S. (1956) Enzymic synthesis of polynucleotides. I. polynucleotide phosphorylase of *Azotobacter vinelandii*. *Biochim. Biophys. Acta* **20,** 269–285 CrossRef Medline
25. Kornberg, A. (1957) Pyrophosphorylases and phosphorylases in biosynthetic reactions. *Adv. Enzymol.* **18,** 191–240 Medline
26. Mason, P. W., Carbone, D. P., Cushman, R. A., and Waggoner, A. S. (1981) The importance of inorganic phosphate in regulation of energy metabolism of *Streptococcus lactis*. *J. Biol. Chem.* **256,** 1861–1866 Medline
27. Libanati, C. M., and Tandler, C. J. (1969) The distribution of the water-soluble inorganic orthophosphate ions within the cell: Accumulation in the nucleus. *J. Cell Biol.* **42,** 754–765 CrossRef Medline